Vietnam Journal of Science and Technology
DOI: https://doi.org/10.15625/2525-2518/21256

Expanded graphite fabricated by rapid induction heating and its application in wastewater treatment

Nguyen Thanh Huong[1], Phung Thi Thu[1], Le Thi Thu Huong[2], Hoang Thi Khuyen[1], Pham Thi Lien[1], Nguyen Vu[1], Nguyen Thi Ngoc Anh[1], Do Khanh Tung[1], Ngo Thi Hong Le[1], Nguyen Thanh Binh[2,*]

[1]*Institute of Materials Science, Vietnam Academy of Science and Technology, 18 Hoang Quoc Viet, Nghia Do ward, Ha Noi, Viet Nam*
[2]*Institute of Physics, Vietnam Academy of Science and Technology, 10 Dao Tan, Giang Vo ward, Ha Noi, Viet Nam*

[*]Email: *binh10m@gmail.com*

Received: 31 July 2024; Accepted for publication: 7 November 2024

Abstract. The increasing global industrial demands have led to water source contamination by hazardous wastes such as organic compounds, dyes, heavy metals, and oils. Consequently, wastewater treatment has become a paramount environmental challenge, requiring efficient, low-cost treatment materials with large-scale manufacturing capabilities. This paper presents a research on synthesizing expanded graphite (EG) materials from graphite intercalation compounds (GIC) using the induction heating method. The properties of the synthesized material have been evaluated through scanning electron microscopy (SEM), specific surface area measurements using the Brunauer-Emmett-Teller (BET) method, X-ray diffraction (XRD), and thermogravimetric analysis (TGA). Additionally, experiments were conducted to evaluate its efficacy in removing dyes such as Methylene Blue (MB) and oils (Diesel Oil - DO) from wastewater. The study results indicate that the synthesized material can adsorb dyes almost completely (> 99 %) and that more than 50 g of diesel oil can be retained by just 1 g of the material. However, there is a difference in the adsorption of hydrophilic and hydrophobic compounds depending on the structure of the EG material. Furthermore, the utilization of the thermal shock synthesis method using an induction furnace demonstrates its capability to produce a large quantity of material at a low cost.

Keywords: expanded graphite, graphite intercalation compounds, thermal shock heating, wastewater treatment, induction furnace.

Classification numbers: 2.4.2, 3.4.2, 3.7.4.

1. INTRODUCTION

Today, environmental pollution due to the increasing development of industries is becoming increasingly serious [1]. Particularly concerning is water pollution caused by hazardous waste such as organic solvents, dyes, heavy metals, and oil spills, which threaten agriculture, aquatic life, and human health [2-4]. In the textile dyeing industry alone, approximately 20 % of the total dyes produced worldwide are regularly discharged into the environment [5]. Petroleum oil has

UNCORRECTED PROOF

been one of the main energy sources worldwide for many decades. It is transported across the oceans and inevitably spills into the sea during many shipwreck accidents. Incidents in the 2010s caused 164,000 tons of oil spills, and oil spills from the 2020s to date have already resulted in a loss of 28,000 tons of oil [6]. These pollutants are not biodegradable, and they accumulate increasingly, harming living organisms and making clean water sources increasingly scarce worldwide. Therefore, the treatment of polluted wastewater sources is a leading environmental challenge. Some techniques have been used to remove harmful substances from wastewater, such as: using membrane filtration [6]; solvent extraction [7]; coagulation-flocculation [8]; chemical precipitation [9]; and adsorption [10-13]. Different types of harmful substances can be appropriately removed by suitable techniques; however, among the aforementioned techniques, the adsorption technique is considered to be highly effective and economical. Various materials such as activated carbon, carbon nanotubes, and graphene have been studied as adsorbents for the removal of pollutants from water. However, the search for highly effective materials that can be produced in large quantities at low cost for practical applications remains a challenge.

Graphene, a 2D carbon nanomaterial discovered in 2004, exhibits outstanding properties such as electrical and thermal conductivity, large specific surface area, high thermal and chemical stability, and is gradually being applied in various fields such as sensors, batteries, supercapacitors, and water purification technology. In recent years, research on graphene-based materials for wastewater treatment has yielded many promising results in terms of fabrication and application potential [14-22]. The production of graphene through graphite intercalation and layer exfoliation has demonstrated the potential to produce graphene at a low cost for applications requiring large quantities of material [23, 24]. In this technique, graphite intercalation compounds (GIC) are typically subjected to thermal shock in an oven, which rapidly evaporates the intercalants, generating a force that separates the graphite layers. The microwave heating method has the advantages of rapid heating speed, uniform temperature, and is commonly used for the fabrication of materials in studies of expanded graphite (EG) properties [23, 25-27]. However, in terms of application, scaling up production using this method is limited due to its complexity and cost. The fabrication of EG can also be carried out in other commonly used furnaces heated by electricity, LPG, Diesel, or radiative heating using IR, UV, such as conventional heating ovens [28-30]. This heating method can be easily scaled up, however, it has drawbacks such as low energy efficiency, slow heating, and uneven temperature distribution. The induction heating method can be seen as a compromise that balances the advantages and disadvantages of the two previous methods. It has the advantages of easy scalability and the ability to be automated, simple, continuous, and safe. This is a novel method in terms of equipment technology, and it has hardly been mentioned in recent reports [27]. In this study, we present the results of synthesizing expanded graphite (EG) materials from GICs, in which the pyrolysis step of GIC was performed using an induction furnace, a device developed at the Institute of Physics, Vietnam Academy of Science and Technology [31]. This approach provides a novel method for the synthesis of EG materials. The characteristics of the synthesized materials were evaluated through scanning electron microscopy (SEM) imaging, specific surface area measurements using the Brunauer-Emmett-Teller (BET) method, X-ray diffraction (XRD), and thermogravimetric analysis (TGA). To assess the capability of removing pollutants from water, experiments on the removal of dyes such as Methylene Blue (MB) and diesel oil (DO) from wastewater were conducted.

UNCORRECTED PROOF

2. MATERIALS AND METHODS

2.1. Materials

Natural graphite powder (NG) sourced from the Yen Bai mine, Viet Nam, with a purity of 96 % and average particle sizes of 300 µm, 180 µm, 100 µm, and 80 µm, equivalent to mesh sizes of 50, 80, 150, and 200 (denoted as NG50, NG80, NG150, NG200), was used as the primary raw material for preparing GIC compounds. The chemicals used for GIC preparation included H_2O_2 (30 %) and H_2SO_4 (98 %), purchased from Merck, along with distilled water. The substances used for testing included anhydrous MB dye (95 %) also purchased from Merck, and commercial DO oil type 0.01S-V.

2.2. Synthesis of EG materials

Before using, the graphite powder was vacuum-dried at 75 °C for 10 hours to remove moisture. The experimental procedure for GIC preparation followed the method described in references [32, 33], with H_2O_2 acting as the oxidizing agent and H_2SO_4 as the intercalating agent. Briefly, 5 g of NG was mixed into a beaker containing 200 ml of H_2O_2 and H_2SO_4 solution at a ratio of 1:15. The solution was stirred for 2 hours, maintaining a temperature below 20 °C until the reaction was complete, as indicated by the cessation of the increase in the reaction volume. The reaction mixture was then filtered and washed multiple times with distilled water until neutral (pH = 7). The filtered GIC powder was vacuum-dried at 80 °C for 24 hours. Based on the different initial particle sizes of NG (NG50, NG80, NG150 and NG200), various GIC compounds were synthesized, denoted as GIC50, GIC80, GIC150 and GIC200, respectively. The GIC powder was then subjected to thermal shock treatment at 550 °C using a custom-built induction furnace in the laboratory [31], resulting in the formation of 2D nanoplatelet samples, also known as EG, designated as EG50, EG80, EG150, and EG200.

2.3. Measurement and evaluation methods

The structural characteristics of the synthesized EG material were evaluated through scanning electron microscopy (SEM) imaging using a Hitachi S-4800 instrument, specific surface area (SSA) analysis using the N_2 adsorption/desorption method (BET - Brunauer-Emmett-Teller) performed on a TriStar II Plus from Micromeritics Instrument Corporation, and X-ray diffraction (XRD) diffractograms measured on a Panalytical Empyrean Instrument. The thermal properties of the material were investigated using a Shimadzu DTG-60H thermogravimetric analyzer (TGA).

The adsorption experiment of MB was conducted at room temperature without any stirring during the process. The MB solution was tested at various concentrations of 10 µmol/L, 20 µmol/L, and 30 µmol/L. The measurement method was as follows: 0.3 g of freshly synthesized EG was soaked in 100 ml of MB solution for durations ranging from 15 to 90 minutes. Afterward, the MB solution was separated from the EG samples by filtration, and the dye removal efficiency was evaluated by measuring the absorbance of the MB solution at a wavelength of 665 nm using a UV-VIS spectrophotometer from Avantes Company. To evaluate the saturated adsorption capacity of the EG material, this procedure was performed similarly to the previous one, summarized as follows: 0.1 g of EG was soaked in 10 ml of 10 mg/L MB solution for 30 minutes. The MB solution was then separated, and its UV-VIS absorbance spectrum was measured. This process was repeated three times, reusing the EG filtered out from the prior cycle. In these

UNCORRECTED PROOF

measurements, the amount of MB adsorbed by the EG sample, expressed in milligrams (M), and as a percentage of the initial amount (P %), are calculated using the following formulas: $M = (C_o - C_i) * V$ and $P = (A_o - A_i)/A_o * 100$ %. Here, C_o and C_i (mg/L) represent the initial concentration and the remaining concentration after each trial, respectively; V is the volume of the solution (L); A_o and A_i correspond to the absorbance of the initial MB solution and after the i^{th} trial, respectively, with the number of trials ranging from i = 1 to 4.

The evaluation of DO adsorption capability was conducted as follows: 1 g of EG sample was immersed in 200 ml of diesel oil (equivalent to 165 g of DO) for 1 hour. Subsequently, a filter bag was used to remove excess DO and retrieve the EG sample after oil absorption. The EG sample was kept in the filter bag for 8 hours before evaluating the absorbed DO amount by weighing the sample and determining the weight increase compared to the initial amount. This experiment was repeated 3 times, and the measured results were averaged. The effect of the simultaneous presence of water and oil on the adsorption capacity of the material has also been investigated. In this experiment, 1 g of the EG50 material was used for adsorption with measurements taken in different compositions: water, oil-to-water ratios of 1:4, 1:2, 1:1, and oil (meaning the percentage of oil in the mixture will correspond to values of 0, 20, 33, 50, and 100 %, respectively). The measurement method was similar to that described above.

The use of EG for removing contaminants from actual wastewater samples from a textile dyeing factory in Viet Nam has also been tested. Untreated wastewater samples were directly collected from the dyeing factory. The experimental process was conducted simply using adsorption at 25 °C with synthesized EG material as the adsorbent. Specifically, 25 ml of wastewater and 0.3 g of EG were placed in a 250 ml beaker and left for 90 minutes. Afterward, filtration was performed to separate the adsorbent from the wastewater. The reuse experiment was repeated 3 times, each time using 25 ml of wastewater under similar conditions as described above.

3. RESULTS AND DISCUSSION

3.1. Structural and physicochemical characteristics of expanded graphite

Results from SEM imaging in Figure 1 clearly depict the morphology of multilayer graphene flakes in the EG samples. The graphene layers exhibit thin, leaf-like structures with good layer separation, and the volume of the EG material after heating has increased hundreds of times compared to the initial GIC volume. At high magnification (Figure 1(b)), multilayer graphene flakes with a thickness of approximately 50 nm can be clearly observed.

The SEM images show that all EG samples (EG50, EG80, EG150, and EG200) exhibit a porous structure formed due to the exfoliation of layers during the thermal shock process. However, the porous structure and voids are most clearly observed in EG50, which is consistent with its highest volume expansion and largest SSA compared to the other samples. The SEM imaging results are consistent with previous findings [32, 33], indicating that the rapid induction heating method is comparable to microwave-assisted thermal shock and confirms the successful synthesis of the desired material.

From the X-ray diffraction patterns of the GIC and EG samples (Figure 2), we can observe that the GIC sample exhibits characteristic peaks with strong intensity at a diffraction angle of 2θ~26°, closely resembling the characteristic peaks of graphite. However, there is a noticeable difference in this case: the peaks are broadened and the intensity is reduced. This variation can be understood as the intercalation process partially expanding the interlayer spacing of the hexagonal

UNCORRECTED PROOF

planes in graphite. The X-ray diffraction spectra obtained from the EG samples after thermal shock treatment show more distinct differences: besides the characteristic peaks of graphite, additional peaks corresponding to graphene structure appear around 2θ~22°. When comparing the intensity ratios of these two peaks, except for the EG150 sample where the trend is not clearly observed, we can see a pattern where the graphene/graphite peak intensity ratio increases in the order of EG200, EG80, and EG50, corresponding to the increase in the expanded volume of EG after thermal shock as well as the increase in their SSA values.

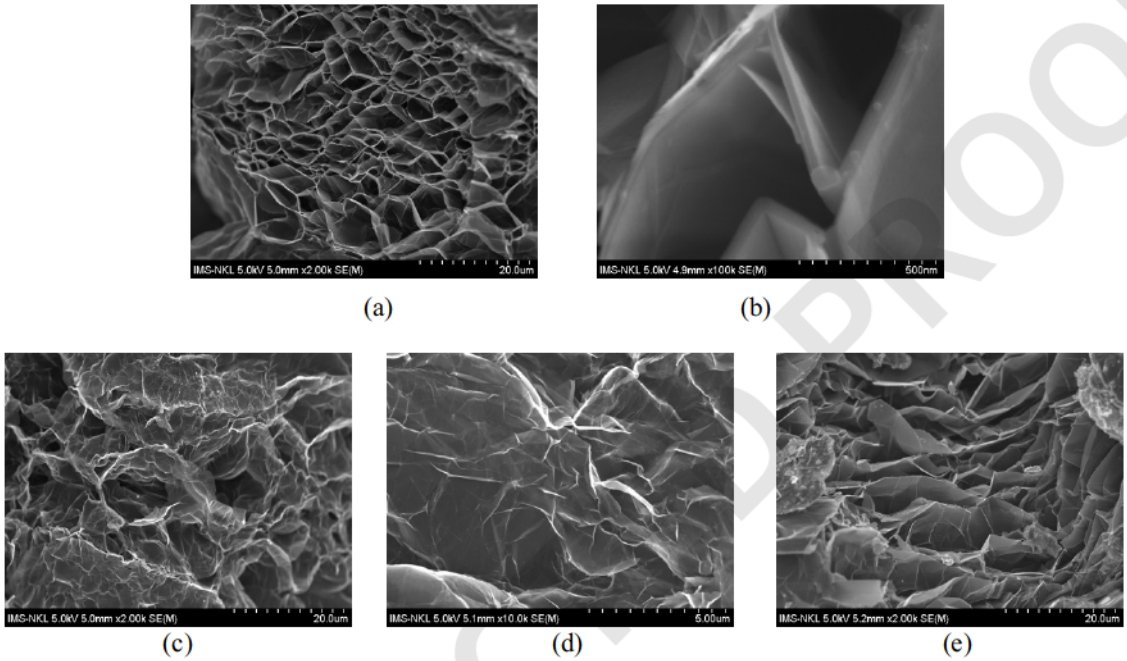

Figure 1. SEM images of EG samples after thermal shock treatment at 550 °C, including samples: EG50 (a) and (b) at higher magnifications, EG80 (c), EG150 (d), and EG200 (e).

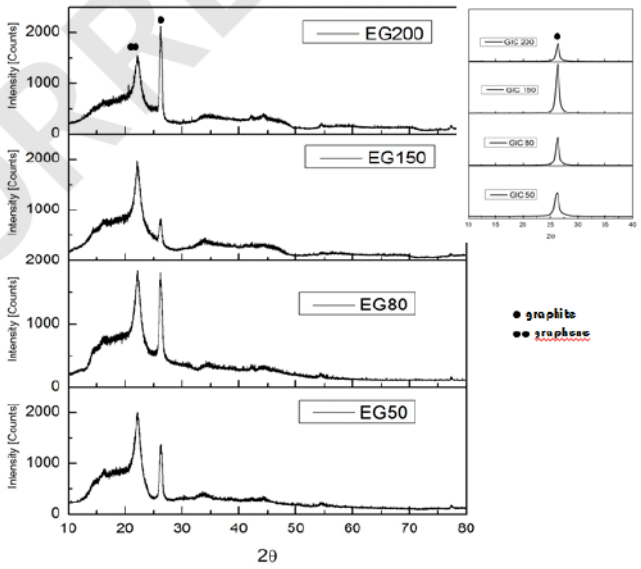

Figure 2. X-ray diffraction patterns of EG samples (left) and GIC samples (right).

UNCORRECTED PROOF

Table 1. Specific surface area (SSA) measurement and parameters related to EG samples.

Parameter	EG50	EG80	EG150	EG200
GIC particle size (µm)	300	180	100	80
SSA (m^2/g)	36	32	22	20

The SSA measurements of the EG samples using the BET method and the parameters related to EG samples are shown in Table 1. The measurement results suggest an apparent paradox: EG materials with a larger specific surface area are not formed from smaller GIC particles, but rather the opposite. However, this is entirely consistent with the published report [34], in which the raw materials with particle sizes of 300, 180, and 150 µm resulted in EG with corresponding SSAs of 34.35, 23.84, and 21.3 m^2/g. This indicates that the exfoliation efficiency during thermal shock is better for larger GIC particles, meaning that more graphene layers are separated from each other. The SSA measurement results also show consistency with some published data: Refs[35] and [36] provide SSA values of 20.3 and 34.3 m^2/g for EG samples with corresponding expansion ratios V (cm^3/g) of 320 and 400, respectively; [25] provides an SSA value of 29.95 m^2/g, and [27] gives an SSA value of 34.8 m^2/g for a V of 300 cm^3/g.

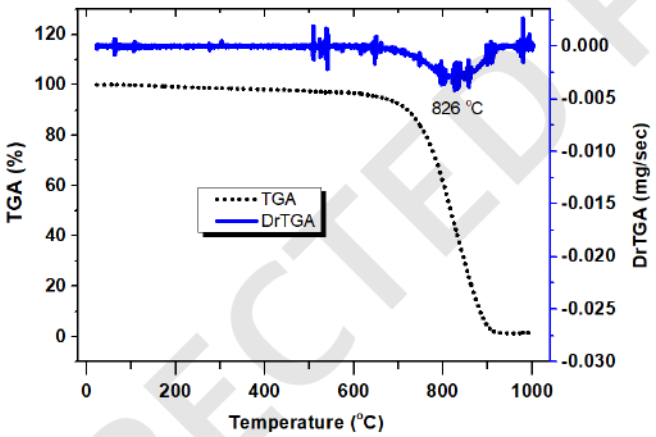

Figure 3. TGA results of the EG50 sample measured in air.

Figure 3 shows the thermogravimetric analysis (TGA) measurement results in air for the EG50 sample. The TGA results indicate that the synthesized EG samples have thermal stability up to over 700 °C. At temperatures below 700 °C, the material is hardly affected, with only the evaporation of impurities amounting to less than 5 %. Around 826 °C, a reaction with oxygen occurs, and at 900 °C, the material is almost completely burned with a 95 % weight loss. Nevertheless, this demonstrates that the material has excellent thermal stability. These TGA results are fully consistent with numerous publications by other authors reporting that the thermal stability of EG can reach temperatures of 800-900 °C [24, 37]. Moreover, many reports have shown that EG can be synthesized under rapid heating conditions, ranging from a few seconds to a few minutes, at a temperature of 800 °C [23], and even at temperatures of 900-1000 °C [30, 34, 35, 38-40].

3.2. Adsorption capacity for the removal of methylene blue (MB)

Figure 4 presents the adsorption measurement results for MB solutions at three concentrations: 10 µmol/L, 20 µmol/L, and 30 µmol/L using four EG samples (EG50, EG80, EG150, and EG200).

UNCORRECTED PROOF

Figure 4(a) shows that the expansion or porosity of the EG produced from the same amount of GIC material increases significantly for larger particle sizes. This is also consistent with the SSA results obtained from BET measurements, as well as the published report [34].

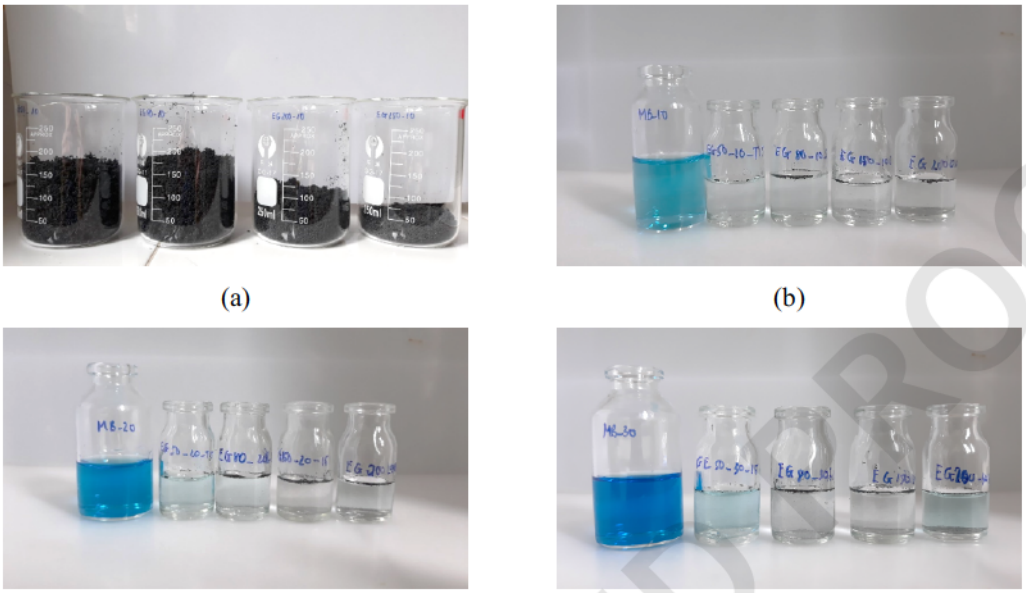

(a) (b)

(c) (d)

Figure 4. Expanded graphite samples (a) and Methylene Blue solutions after soaking with EG samples for 15 minutes at concentrations of 10 µmol/L (b), 20 µmol/L (c), and 30 µmol/L (d).

The adsorption experimental results show that the EG samples adsorb MB quite rapidly. For all three tested MB concentrations, upon adding the EG material, the solution's color quickly faded, becoming nearly transparent within just 15 minutes. With longer soaking times, MB was adsorbed more strongly, making it difficult to visually distinguish the color change in the MB solution. These observations were then quantitatively conducted by UV-VIS absorption measurements, which will be discussed in the following section.

The MB solution samples after the adsorption process were filtered to remove solid residues and used to assess the remained MB concentration through absorbance measurements at the characteristic wavelength of 665 nm (Figure 5). In Figure 5(d), the results of adsorption for the 10 µmol/L MB solution are also presented, using different masses of adsorbents EG80 and EG150.

From these results, it is evident that the amount of MB adsorbed increases over soaking time and with the amount of adsorbent used, showing a tendency toward saturation. The adsorption capacity of MB varies among the EG samples and tends to increase in the order of EG50, EG80, EG150, and EG200. When compared to the BET results above (Table 1), these findings appear contradictory because the EG samples, which have larger specific surface areas, exhibit lower MB adsorption capacity, and vice versa. Therefore, it can be asserted that the specific surface area of EG is not the determining factor in adsorption of MB in aqueous solutions. Another study has also shown that there is a difference in the adsorption positions of hydrophobic substances (such as oil) and hydrophilic substances (such as PEG) on the structure of EG, where oil tends to fill the pores while PEG is located at the edges or defect sites on the surface [28]. This report also confirms that the adsorption mechanisms of oil and PEG are different, however, the author only

UNCORRECTED PROOF

used one type of EG, so the impact of particle size on the adsorption capacity of hydrophilic substances has not been clearly evaluated. Previous research results [39] suggest that the high-temperature fabrication process of EG leads to the formation of oxygen functional groups located at the edges of the graphite crystal. Therefore, samples with structures that have a larger edge area increase their wettability. The EG surface is hydrophobic, making it difficult for water to adhere to the surface or penetrate into the pores. However, the author [39] also suggests that, depending on the fabrication conditions during the exfoliation process, the material may form more or fewer carbon defect fragments on the surface with oxygen groups, which will increase or decrease the surface wettability.

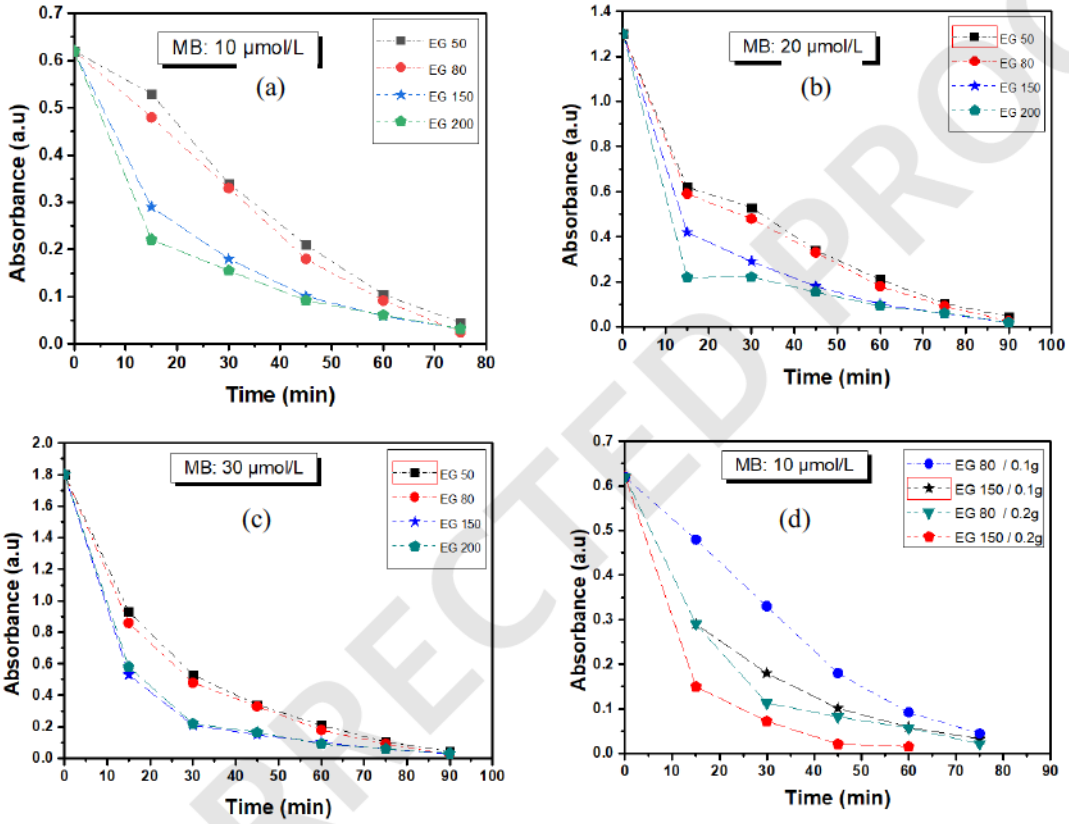

Figure 5. Decrease in MB solution concentration over soaking time from 15 to 90 minutes, with initial concentrations of 10 µmol/L (a), 20 µmol/L (b), and 30 µmol/L (c), and the effect of varying amounts of adsorbent EG (d). Measurements were conducted at room temperature, with 0.3 g of adsorbent EG and 100 mL of MB solution.

We also know that MB is a hydrophilic compound and readily soluble in water, so in our study, it is likely that MB will be more effectively adsorbed at the positions located at the edges of EG flakes. This is a reasonable explanation because with the same sample mass, the ratio of edge area to surface area of 2D EG flakes increases as the flake size decreases. This means that this ratio increases in the order of EG50, EG80, EG150, and EG200 samples. Furthermore, the amount of adsorbed MB does not increase with the SSA values of these samples, suggesting that the carbon defect fragments on the surface with oxygen functional groups are sufficiently few and play a minor role in the adsorption of MB.

UNCORRECTED PROOF

Aiming to study the reusability of graphene, the MB adsorption capacity was measured in four consecutive trials. The results are summarized in Table 2 and indicate that the synthesized EG material can adsorb the MB dye almost completely (> 99 %) in the first and second trials (with an adsorption capacity of about 1 mg/g). In the subsequent trials, the amount of MB adsorbed tends to decrease, but it is evident that this material has excellent MB adsorption efficiency and can be reused multiple times. In this experiment, a relatively small amount of adsorbate (MB) to adsorbent (EG) ratio was used to evaluate the continuous reusability of EG. However, according to some other reports, when this ratio is increased, the percentage of MB adsorbed tends to decrease, and the amount of MB adsorbed tends to reach a maximum. For example, 0.1 g of the EG compound can capture about 68.2% of MB from a 10 mL solution with a concentration of 50 mg/L, resulting in an adsorption capacity of approximately 3.4 mg/g [37]. Alternatively, using EG samples with an SSA of 29.95 m^2/g at a concentration of 2 g/L for MB adsorption at a concentration of 200 mg/L yielded results of 41.92 % and 83.8 mg/g, respectively [25].

Table 2. The percentage (P %) and the amount (M mg) of methylene blue adsorbed by the EG200 sample, measured over four consecutive reuse cycles for 30 minutes at room temperature, using 10 mL of 10 mg/L MB solution and 0.1 g of EG.

No.	Adsorbed methylene blue	
	P (%)	M (mg)
0	0	0
1	99.9	0.0999
2	99.8	0.0997
3	98.2	0.0982
4	87.6	0.0876

3.3. Investigation of the diesel oil adsorption capacity of graphene

The results of the study on the oil adsorption capacity of graphene are presented in Figure 6. To evaluate the DO adsorption capacity of the EG samples. The oil-adsorbed samples were filtered and weighed to determine the amount of oil adsorbed. These results, along with the SSA data of the EG samples, are presented in Figure 6(a). Another result measuring the amounts of oil and water adsorbed by 1 g of the EG50 sample in the simultaneous presence of both components at oil/water ratios of 0, 20, 33, 50, and 100 % is shown in Figure 6(b).

From these results, it can be seen that EG materials have a good oil adsorption capacity, with values ranging from 30 to over 50 g of oil retained per 1 g of material. Notably, the oil adsorption capacity decreases with the reduction in specific surface area (SSA) of the material (i.e., in the order of EG50, EG80, EG150, and EG200), which is contrary to the MB adsorption results mentioned above. This difference is attributed to the fact that, unlike MB, oil has hydrophobic properties. Additionally, as noted in the MB adsorption measurements above, the hydrophobic surface area contributing to the total SSA of the EG material decreases in the same order, leading to a reduction in the amount of oil retained. Moreover, previous studies have shown that the significant amount of oil absorbed by EG is due to the oil being adsorbed and filling the pores of the porous structure [28].

From the results in Figure 6(b), we can observe that EG materials also exhibit water absorption capability, but significantly less compared to oil absorption (11 g of water versus 51 g of oil absorbed per 1 g of material). However, the water adsorption capacity is quite similar to the results

UNCORRECTED PROOF

reported in a recent study for EG fabricated from graphite with particle sizes ranging from 200 to 300 µm, showing a sorption capacity of 11 to 16 g/g [39]. Graphene materials exhibit a preference for oil adsorption due to their hydrophobic surface advantage. EG and graphene materials are classified as high-capacity oil adsorbents, achieving values from 50 to 70 g/g [27], thanks to their porous structure and significantly larger SSA compared to natural graphite and GIC compounds, which have an SSA in the range of 1.0–1.22 m^2/g [41, 42]. The results in Figure 6(b) clearly show that increasing the oil/water ratio leads to a rapid increase in the total adsorbed substance. However, at higher oil/water ratios (above 33 %), the total weight of adsorbed substance decreases. This can be attributed to saturation of the adsorption sites where oil tends to displace previously adsorbed water molecules. Additionally, the lower density of oil compared to water results in a reduction in the measured total weight. The oil adsorption capacity measured in this study is nearly achieved and quite similar to the results reported in some published studies. For example, the oil (n-dodecane) adsorption capacity of EG and natural graphite is 47 g/g and 7 g/g, respectively, and this significant difference is due to the large SSA and porous structure of the EG [38]. Additionally, as reported in [27, 38], EG can adsorb 42.12 and 37.26 g/g of DO, respectively.

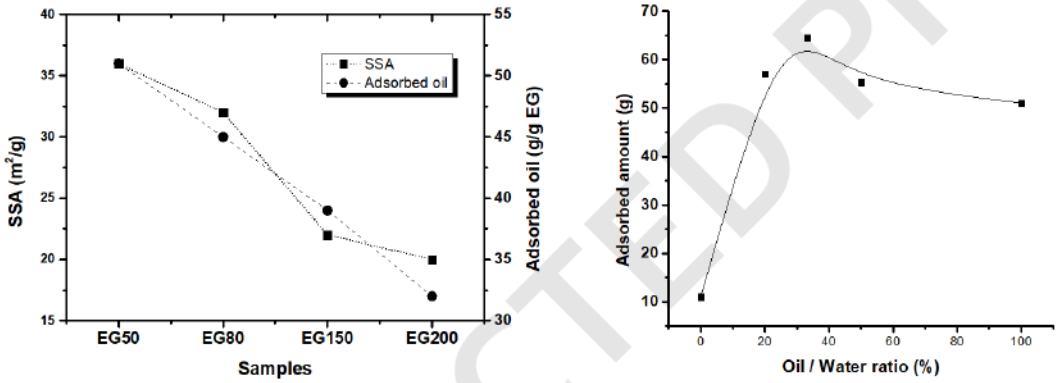

(a) (b)

Figure 6. Comparison between SSA and oil retention capacity of EG samples (a), and the amount of substance adsorbed by the EG50 sample in the presence of both oil and water components (b).

3.4. Expanded graphite's capability in treating textile dyeing wastewater

Results of treating textile dye wastewater with EG200 material for 90 minutes are presented in Figure 7. It is evident that the collected wastewater appears black with high pH (pH = 11-12). After treatment, the resulting solution becomes colorless and transparent, with pH significantly reduced to approximately 8. Clearly, the colorants and pH components present in the initial wastewater were effectively removed in the presence of graphene in the water.

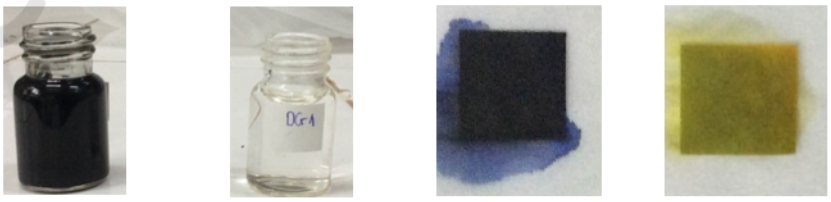

(a) (b) (c) (d)

Figure 7. Initial wastewater (a), wastewater after 90-minute treatment with EG200 (b), pH of the corresponding wastewater before and after treatment (c) and (d).

UNCORRECTED PROOF

Figure 8 shows the results of UV-VIS absorption spectra of wastewater before and during treatment with graphene material. The initial wastewater is labeled as Dye0, and subsequent treatments are labeled correspondingly as Dye1, Dye2, Dye3, and Dye4, indicating repeated processing trials. The initial textile dye wastewater exhibits a broad spectrum from ultraviolet to visible regions, with two main peaks at wavelengths 476 nm and 590 nm. As seen in Figure 8, the color-causing pollutants in the wastewater are almost completely absorbed, achieving 97.7 % removal in the first treatment (Dye1), reflected in the colorless and transparent appearance of the treated water.

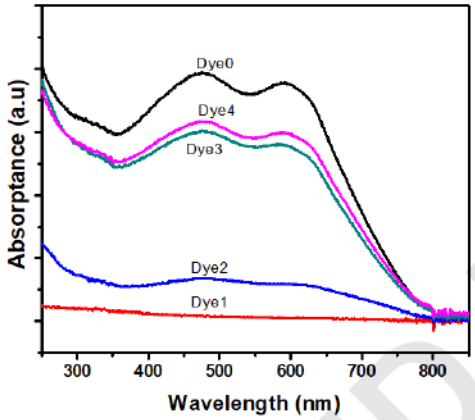

Figure 8. UV-VIS spectra of the initial wastewater Dye0 and the four consecutive treatment trials labeled as Dye1, Dye2, Dye3, and Dye4.

The multiple measurements aim to determine the saturation adsorption capacity and reusability of the material. In the first reuse cycle (Dye2), the amount of textile dye in the wastewater was reduced to approximately 17 %. After this cycle, having adsorbed an additional 83 % of the dye compound, the graphene's adsorption capacity became nearly saturated in subsequent trials. This is evident in the third and fourth experiments, where the adsorption capacity significantly decreased, resulting in a much smaller amount of contaminants being removed, specifically 23.5 % and 19.5 %, respectively. This experiment also showed that to reuse the materials and maintain their adsorption capacity for removing contaminants from water, it is necessary to remove the previously adsorbed substances from the adsorbent. Based on the thermal stability of up to 700 °C (as shown by the TGA results in Figure 3), the thermal regeneration method can be advantageous for this type of material because organic contaminants, having much lower thermal stability, can be completely burned off without affecting the adsorbent.

4. CONCLUSIONS

The results of this study demonstrated that expanded graphite materials can be fabricated by exfoliating GIC using thermal shock treatment. This is a physical method with relatively simple technology that allows for scalable production at a low cost. Notably, the thermal shock technique using an induction furnace offers advantages over microwave heating in terms of simpler design, ease of automation, and the ability to maintain continuous production processes. The measurement data showed that 2D expanded graphite materials obtained from the initial GIC, with different flake sizes of 50, 80, 150, and 200 mesh (designated as EG50, EG80, EG150, and EG200), were successfully fabricated. The study results on the adsorption capacity of MB dye and DO demonstrated that the fabricated materials have excellent retention abilities. Specifically,

UNCORRECTED PROOF

the EG200 material can capture over 99 % of MB in water during its first use, and 1 g of EG50 material can retain over 50 g of DO. The fabricated material also demonstrated the ability to remove both hydrophilic compounds (such as MB) and hydrophobic compounds (such as DO) from wastewater. However, there is a difference in the adsorption of hydrophilic and hydrophobic compounds depending on the structure of the graphene material. Specifically, it is believed to be influenced differently by the 2D hexagonal carbon surface area and the edges of the graphene flakes. For the removal of compounds similar to MB, the edges play a more dominant role than the surface area, whereas for hydrophobic compounds like DO, the opposite is true. These observations provide guidance for tailoring graphene materials to remove contaminants with different properties.

Acknowledgements. This research was funded by the Vietnam Academy of Science and Technology under grant number KHCBVL.02/23-24.

CRediT authorship contribution statement. Nguyen Thanh Huong: Methodology, Investigation, Funding acquisition. Phung Thi Thu: Methodology, Investigation. Le Thi Thu Huong, Hoang Thi Khuyen, Pham Thi Lien, Nguyen Vu: Investigation, Formal analysis. Nguyen Thi Ngoc Anh, Do Khanh Tung, Ngo Thi Hong Le: Investigation. Nguyen Thanh Binh: Supervision, Writing – review & editing.

Declaration of competing interest. The authors declare that they have no known competing financial interests or personal relationships that could have appeared to influence the work reported in this paper.

REFERENCES

1. Mishra K., Siwal S. S., Nayaka S. C., Guan Z., Thakur V. K. - Waste-to-chemicals: Green solutions for bioeconomy markets. Sci. Total Environ., **887** (2023) 164006. https://doi.org/10.1016/j.scitotenv.2023.164006.
2. Chowdhury S., Uddin M. E., Noyon M. A. R., Mondol M. M. H., Maafa I. M., Yousef A. - Fabrication and performance analysis of keratin based-graphene oxide nanocomposite to remove dye from tannery wastewater. Heliyon, **10**(1) (2023) e23421. https://doi.org/10.1016/j.heliyon.2023.e23421.
3. Afroze S., Sen T. K. - A Review on Heavy Metal Ions and Dye Adsorption from Water by Agricultural Solid Waste Adsorbents. Water Air Soil Pollut., **229**(7) (2018) https://doi.org/10.1007/s11270-018-3869-z.
4. Tabish T. A., Memon F. A., Gomez D. E., Horsell D. W., Zhang S. - A facile synthesis of porous graphene for efficient water and wastewater treatment. Sci. Rep., **8**(1) (2018) 1817. https://doi.org/10.1038/s41598-018-19978-8.
5. Hanafi M. F., Sapawe N. - A review on the water problem associate with organic pollutants derived from phenol, methyl orange, and remazol brilliant blue dyes. Mater. Today Proc., **31** (2021) A141-A150. https://doi.org/10.1016/j.matpr.2021.01.258.
6. Chen M., Heijman S. G. J., Rietveld L. C. - Ceramic membrane filtration for oily wastewater treatment: Basics, membrane fouling and fouling control. Desalination, **583** (2024) 117727. https://doi.org/10.1016/j.desal.2024.117727.
7. Hu G., Li J., Hou H. - A combination of solvent extraction and freeze thaw for oil recovery from petroleum refinery wastewater treatment pond sludge. J. Hazard. Mater., **283** (2015) 832-840. https://doi.org/10.1016/j.jhazmat.2014.10.028.
8. Ihaddaden S., Aberkane D., Boukerroui A., Robert D. - Removal of methylene blue (basic dye) by coagulation-flocculation with biomaterials (bentonite and Opuntia ficus indica). J. Water Process Eng., **49** (2022) 102952. https://doi.org/10.1016/j.jwpe.2022.102952.
9. Oh M., Lee K., Jeon M. K., Foster R. I., Lee C. H. - Chemical precipitation-based treatment of acidic wastewater generated by chemical decontamination of radioactive concrete. J. Environ. Chem. Eng., **11**(5) (2023) 110306. https://doi.org/10.1016/j.jece.2023.110306.

UNCORRECTED PROOF

10. Wang W., Tian G., Wang D., Zhang Z., Kang Y., Zong L., Wang A. - All-into-one strategy to synthesize mesoporous hybrid silicate microspheres from naturally rich red palygorskite clay as high-efficient adsorbents. Sci. Rep., **6** (2016) 39599. https://doi.org/10.1038/srep39599.
11. Ali I. - New generation adsorbents for water treatment. Chem. Rev., **112**(10) (2012) 5073-5091. https://doi.org/10.1021/cr300133d.
12. Oladoye P. O., Kadhom M., Khan I., Hama Aziz K. H., Alli Y. A. - Advancements in adsorption and photodegradation technologies for Rhodamine B dye wastewater treatment: Fundamentals, applications, and future directions. Green Chem. Eng., **5**(4) (2023) 440-460. https://doi.org/10.1016/j.gce.2023.12.004.
13. Khader E. H., Khudhur R. H., Mohammed T. J., Mahdy O. S., Sabri A. A., Mahmood A. S., Albayati T. M. - Evaluation of adsorption treatment method for removal of phenol and acetone from industrial wastewater. Desalin. Water Treat., **317** (2024) 100091. https://doi.org/10.1016/j.dwt.2024.100091.
14. Sheoran K., Kaur H., Siwal S. S., Saini A. K., Vo D. N., Thakur V. K. - Recent advances of carbon-based nanomaterials (CBNMs) for wastewater treatment: Synthesis and application. Chemosphere, **299** (2022) 134364. https://doi.org/10.1016/j.chemosphere.2022.134364.
15. Malhotra M., Puglia M., Kalluri A., Chowdhury D., Kumar C. V. - Adsorption of metal ions on graphene sheet for applications in environmental sensing and wastewater treatment. Sens. Actuators Rep., **4** (2022) 100077. https://doi.org/10.1016/j.snr.2022.100077.
16. Janani R., Gurunathan B., Sivakumar K., Senthilkumar P. - Strychnos potatorum seeds derived magnetic graphene oxide nanocomposite for removal of nickel from wastewater: Adsorption performance, isotherm, kinetic and desorption behavior. Desalin. Water Treat., **319** (2024) 100463. https://doi.org/10.1016/j.dwt.2024.100463.
17. Youssef Z., Colombeau L., Yesmurzayeva N., Baros F., Vanderesse R., Hamieh T., Toufaily J., Frochot C., Roques-Carmes T., Acherar S. - Dye-sensitized nanoparticles for heterogeneous photocatalysis: Cases studies with TiO2, ZnO, fullerene and graphene for water purification. Dyes Pigm., **159** (2018) 49-71. https://doi.org/10.1016/j.dyepig.2018.06.002.
18. Lai K. C., Lee L. Y., Hiew B. Y. Z., Thangalazhy-Gopakumar S., Gan S. - Environmental application of three-dimensional graphene materials as adsorbents for dyes and heavy metals: Review on ice-templating method and adsorption mechanisms. J. Environ. Sci., **79** (2019) 174-199. https://doi.org/10.1016/j.jes.2018.11.023.
19. Kyzas G. Z., Deliyanni E. A., Bikiaris D. N., Mitropoulos A. C. - Graphene composites as dye adsorbents: Review. Chem. Eng. Res. Des., **129** (2018) 75-88. https://doi.org/10.1016/j.cherd.2017.11.006.
20. Abu-Nada A., Abdala A., McKay G. - Removal of phenols and dyes from aqueous solutions using graphene and graphene composite adsorption: A review. J. Environ. Chem. Eng., **9**(5) (2021) 105858. https://doi.org/10.1016/j.jece.2021.105858.
21. Shah I. A., Bilal M., Ihsanullah I., Ali S., Yaqub M. - Revolutionizing water purification: Unleashing graphene oxide (GO) membranes. J. Environ. Chem. Eng., **11**(6) (2023) 111450. https://doi.org/10.1016/j.jece.2023.111450.
22. Rana K., Kaur H., Singh N., Sithole T., Siwal S. S. - Graphene-based materials: Unravelling its impact in wastewater treatment for sustainable environments. Next Mater., **3** (2024) 100107. https://doi.org/10.1016/j.nxmate.2024.100107.
23. Kunene P. N., Mahlambi P. N., Ndlovu T. - Adsorption of antiretroviral drugs, abacavir, nevirapine, and efavirenz from river water and wastewater using exfoliated graphite: Isotherm and kinetic studies. J. Environ. Manage., **360** (2024) 121200. https://doi.org/10.1016/j.jenvman.2024.121200.
24. Momodu D., Madito M. J., Singh A., Sharif F., Karan K., Trifkovic M., Bryant S., Roberts E. P. L. - Mixed-acid intercalation for synthesis of a high conductivity electrochemically exfoliated graphene. Carbon, **171** (2021) 130-141. https://doi.org/10.1016/j.carbon.2020.08.066.
25. Hoang N. B., Nguyen T. T., Nguyen T. S., Bui T. P. Q., Bach L. G., Duc N. D. - The application of expanded graphite fabricated by microwave method to eliminate organic dyes in aqueous solution. Cogent Eng., **6**(1) (2019) 1584939. https://doi.org/10.1080/23311916.2019.1584939.
26. Tarango-Rivero G., Mendoza-Duarte J. M., Santos-Beltrán A., Estrada-Guel I., Garay-Reyes C. G., Pizá-Ruiz P., Gómez-Esparza C. D., Rocha-Rangel E., Martínez-Sánchez R. - Effect of process

UNCORRECTED PROOF

parameters on the graphite expansion produced by a green modification of the Hummers method. Molecules, **27**(21) (2022) https://doi.org/10.3390/molecules27217399.
27. Elbidi M., Mohd Salleh M. A., Rashid S. A., Mukhtar Gunam Resul M. F. - The potential of thermally expanded graphite in oil sorption applications. RSC Adv., **14**(23) (2024) 16466-16485. https://doi.org/10.1039/D4RA00049H.
28. Pang X. Y. - Adsorption capacity and mechanism of expanded graphite for polyethylene glycol and oils. J. Chemistry, **7**(4) (2010) 1258-1265. https://doi.org/10.1155/2010/565468.
29. Pang X. Y., Gong F. - Study on the adsorption kinetics of Acid Red 3B on expanded graphite. J. Chemistry, **5**(4) (2008) 802-809. https://doi.org/10.1155/2008/786025.
30. Pang X. Y., Lv P., Feng Y. Q., Liu X. W. - Study on the adsorbing characteristics of expanded graphite for organic dyes. Environ. Sci.: Indian J., **3**(2) (2008) 150-157.
31. Binh N. T., Tuan A. D., Tinh N. T., Hai H. M. - Method and apparatus for fabricating multilayer graphene nanosheets from graphite compound. 34682, VN Patent (2022).
32. Binh N. T., Dung N. D., Tinh N. T., Huynh M. D., Giang N. V. - Study on the properties of graphite nanoplatelets fabricated from natural graphite of Vietnam. Proc. SPMS2015, (2015) 498.
33. Binh N. T., Dung N. D., Huong N. T. M., Huong L. T. T., Tinh N. T. - Study on the fabrication of multi-layer graphene materials for application in electrically conductive polymer composites. Proc. SPMS2017, (2017) 899.
34. Pang X. Y., Ren S. X., Di X., Sun S. Y. - Study on the competitive adsorption performance of Direct Deep Blue and Methyl Orange on expanded graphite adsorbent. Res. Rev.: J. Ecol. Environ. Sci., **2**(1) (2014) 23-32.
35. Pang X. - Study on the discolored thermodynamics of dyes on expanded graphite loaded with Titania. Int. J. ChemTech Res., **2**(2) (2010) 1281-1288.
36. Pang X., Yang C., Ren S. - Adsorption capacity of expansion graphite for xylenol orange. J. Mater. Sci. Chem. Eng., **1**(1) (2013) 1-5. https://doi.org/10.4236/msce.2013.11001.
37. Tian Y., Zhang N., Liu Y., Chen W., Lv R., Ma H. - Adsorption performance of expanded graphite and its binary composite microbeads toward oil and dyes. Desalin. Water Treat., **178** (2020) 283-295. https://doi.org/10.5004/dwt.2020.24937.
38. Park S. J., Lee S. Y., Kim K. S., Jin F. L. - A novel drying process for oil adsorption of expanded graphite. Carbon Lett., **14**(3) (2013) 193-195. https://doi.org/10.5714/CL.2013.14.3.193.
39. Ivanov A. V., Divitskaya D. A., Lavrin M. A., Kravtsov A. V., Volkova S. I., Maksimova N. V., Kalachev I. L., Kirichenko A. N., Rodionov N. B., Malakho A. P., Avdeev V. V. - Exfoliated graphite for sorption of liquid hydrocarbons from the water surface: Effect of preparation conditions on sorption capacity and water wettability. Adsorption, **30**(6) (2024) 755-767. https://doi.org/10.1007/s10450-024-00475-6.
40. Wang G., Sun Q., Zhang Y., Fan J., Ma L. - Sorption and regeneration of magnetic exfoliated graphite as a new sorbent for oil pollution. Desalination, **263**(1-3) (2010) 183-188. https://doi.org/10.1016/j.desal.2010.06.056.
41. Ahmad A., Kanwal M., Qaisrani N. A., Arshad F., Akram N. - Industrial wastewater treatment by using graphite intercalation compounds as an adsorbent. Iran. J. Chem. Chem. Eng., **42**(11) (2023) 3683-3696. https://doi.org/10.30492/ijcce.2023.1987588.5818.
42. Hussain S. N. - Water treatment using graphite adsorbents with electrochemical regeneration. The University of Manchester (2012).

UNCORRECTED PROOF